THE JOURNAL OF PHYSICAL CHEMISTRY B

Article

pubs.acs.org/JPCB

Investigation of Acrylic Acid at High Pressure Using Neutron Diffraction

Blair F. Johnston,[†] William G. Marshall,[‡] Simon Parsons,[§] Andrew J. Urquhart,[∥] and Iain D. H. Oswald*[,†]

[†]Strathclyde Institute of Pharmacy and Biomedical Sciences, University of Strathclyde, 161 Cathedral Street, Glasgow, U.K., G4 0RE

[‡]ISIS Neutron and Muon Source, Science and Technology Facilities Council, Rutherford Appleton Laboratory, Harwell Oxford, Didcot, Oxon, U.K., OX11 0QX

[§]School of Chemistry and Centre for Science at Extreme Conditions, University of Edinburgh, King's Buildings, West Mains Road, Edinburgh, U.K., EH9 3JJ

[∥]Department of Micro- and Nanotechnology, Building 345Ø, Ørsteds Plads, Technical University of Denmark, 2800 Kgs. Lyngby, Denmark

Supporting Information

ABSTRACT: This article details the exploration of perdeuterated acrylic acid at high pressure using neutron diffraction. The structural changes that occur in acrylic acid-d_4 are followed via diffraction and rationalized using the Pixel method. Acrylic acid undergoes a reconstructive phase transition to a new phase at ∼0.8 GPa and remains molecular to 7.2 GPa before polymerizing on decompression to ambient pressure. The resulting product is analyzed via Raman and FT-IR spectroscopy and differential scanning calorimetry and found to possess a different molecular structure compared with polymers produced via traditional routes.

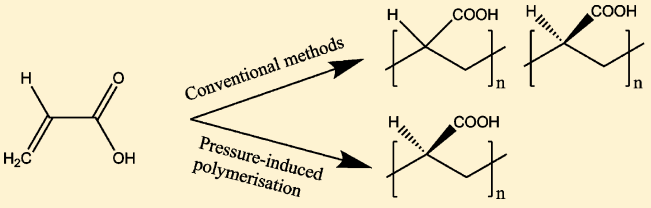

INTRODUCTION

High-pressure techniques have been successfully employed to investigate the polymorphism of a number of different molecular organic solids.[1−4] The exploration using high-pressure techniques allows for a greater range of phase space to be investigated for new polymorphs of materials. The observation of polymorphism at high pressure is an important factor for the exploration of polymerization, as different three-dimensional arrangements of molecules will have an effect on the structure of the polymer that is produced. A number of groups have been investigating the use of high pressure (1−100 GPa) to investigate the chemical reaction of a number of systems via the crystalline state[5] including simple systems such as ethylene,[6] benzene,[7] and even CO_2.[8] As an example of the pressures required to induce chemical reactions, Chelazzi and co-workers subjected ethylene to ∼3.0 GPa to produce polyethylene, while Santoro and co-workers observed the transition of CO_2 into an amorphous nonmolecular phase between 40 and 48 GPa. Further examples include a number of acetylene derivatives.[9−14] Many of these studies have used spectroscopic techniques to elucidate the changes in structure before and after the polymerization reaction.

A recent and novel extension of the work is to combine polymerization with crystal engineering, the ability to manipulate intermolecular interactions to create multicomponent materials.[15,16] By using crystal engineering strategies, Goroff's team manipulated intermolecular interactions between oxalamides and diiodobutadiyne to ensure that the carbon−carbon triple bonds of diiodobutadiyne aligned in a specific manner so as to aid the pressure-induced polymerization process. By doing so, the authors followed the polymerization process, including changes to the crystalline state, via X-ray diffraction due to the maintenance of long-range order in the overall structure. Further work has extended the investigation of high-pressure polymerization to ring systems such as L,L-lactide[17] and carnosine.[18]

In this article, we have investigated the room-temperature behavior of acrylic acid (Scheme 1) at high pressure using neutron diffraction. Acrylic acid is the simplest unsaturated carboxylic acid and is the precursor to poly(acrylic acid) (PAA). PAA is used in a wide range of research and industrial applications, ranging from superabsorbent materials to drug delivery vehicles.[19] Recent studies by Murli and Song[20] and our own group[21] have investigated acrylic acid-h_4 under high-pressure conditions and have revealed the existence of the new

Scheme 1. Numbering Scheme for Acrylic Acid-d_4

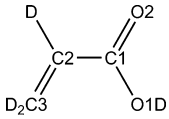

Received: February 28, 2014
Revised: March 20, 2014
Published: March 20, 2014

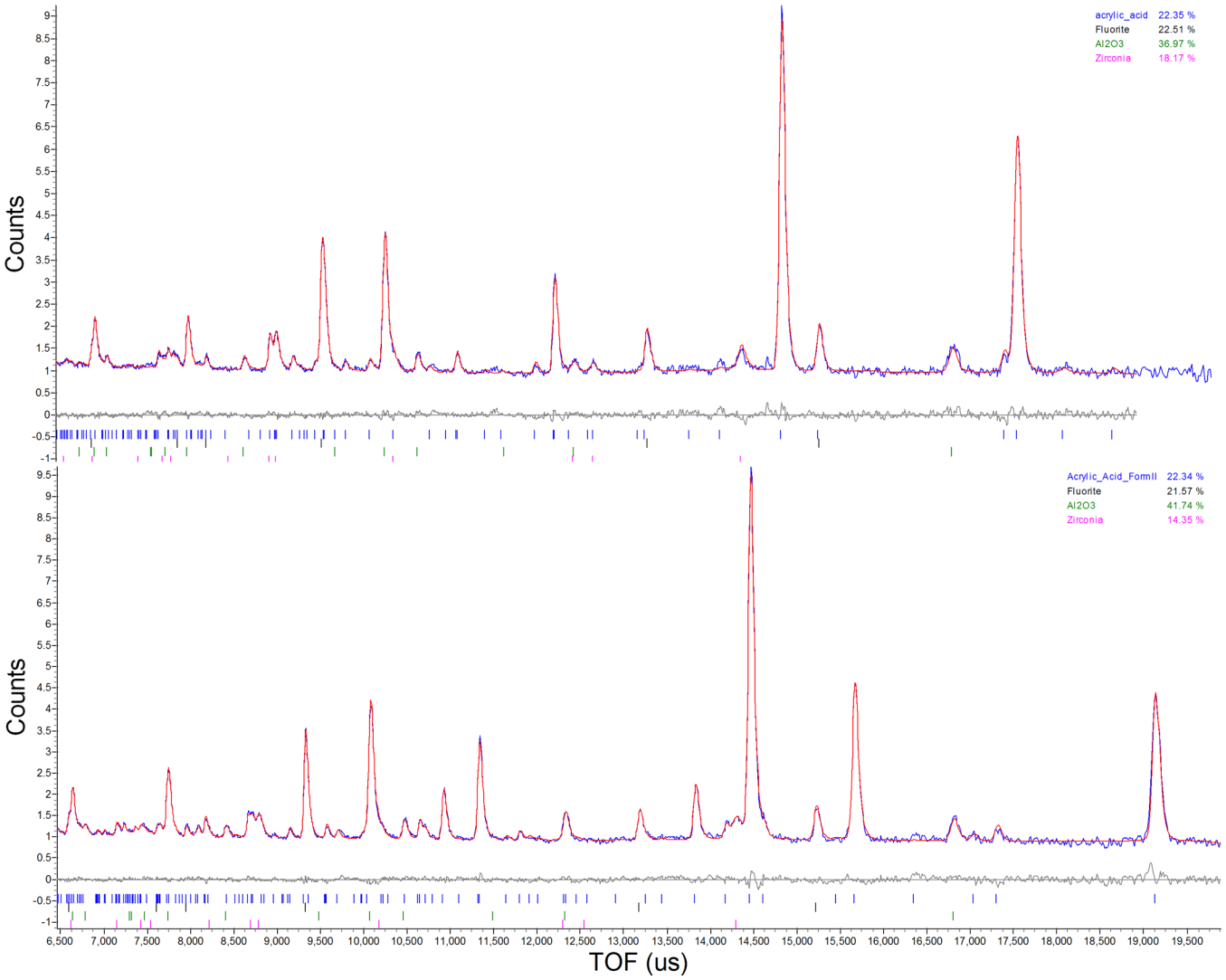

Figure 1. The Rietveld refinements of phase I at 0.33 GPa (upper) and phase II at 0.87 GPa (lower).

polymorph of pure acrylic acid by rapid compression to 3.3 GPa or through the use of a solution of acrylic acid in a pressure transmitting medium (PTM) of 4:1 methanol:ethanol (50% v/v) at 0.61 GPa. The discovery of a new polymorph at high pressure is an important finding, as the spatial arrangement of molecules in the crystal structure may have a significant effect on the structure of the polymer that is created via this polymorph. In our own work, there was an indication that the X-ray radiation was in fact polymerizing the material, as the diffraction pattern started to deteriorate after 15 h of data collection. For this reason, we decided to investigate the changes that occur to the crystal structure before the polymerization process via neutron diffraction due to its noninvasive nature. Herein, we present the results of this study, as well as further spectroscopic analysis of the polymerization product.

EXPERIMENTAL SECTION

Neutron Diffraction Measurements. High-pressure neutron powder diffraction data were collected for acrylic acid-d_4 using the *PEARL* diffractometer[22,23] at the U.K. spallation neutron source, ISIS, located at the STFC Rutherford Appleton Laboratory. Neutron data associated with the research published in this paper can be requested from the corresponding author. Perdeuteration is required to avoid the large backgrounds that would be observed in hydrogenous materials due to the large incoherant scattering cross section of hydrogen. As a point of note, there have been a number of studies that have explored the use of neutron diffraction for the hydrogenous materials to negate the requirement to deuterate samples.[24,25] The sample was first mixed with ∼20% 4:1 methanol-d_4:ethanol-d_6 before being added dropwise using a glass capillary into a standard Ti−Zr alloy capsule gasket[26] filled with loosely packed ground silica wool which was used to inhibit the formation of large crystallites. The methanol:ethanol mixture was used as a PTM to provide quasi-hydrostatic conditions during the compression. Calcium fluoride was mixed with the silica wool to act as a suitable pressure marker. The resulting capsule assembly was then compressed within a type V3b Paris-Edinburgh (P-E) press[27] equipped with standard profile anvils with cores fabricated from zirconia toughened alumina (ZTA). The P-E cell ram pressure was monitored and controlled by means of an automated hydraulic system.

Time-of-flight (TOF) neutron powder diffraction data suitable for structure refinement were obtained by electronically focusing the 702 individual detector element spectra of the

dx.doi.org/10.1021/jp502095n | J. Phys. Chem. B 2014, 118, 4044−4051

Table 1. Crystallographic Information for the Lowest and Highest Pressure Rietveld Refinements for Phase I and Phase II of Acrylic Acid-d_4

CIF ID	1	3	4	19
pressure (GPa)	0.33	0.69	0.87	7.21
chemical formula	$C_3D_4O_2$	$C_3D_4O_2$	$C_3D_4O_2$	$C_3D_4O_2$
M_r	76.07	76.07	76.07	76.07
radiation type	TOF neutron	TOF neutron	TOF neutron	TOF neutron
phase	I	I	II	II
cell setting, space group	orthorhombic, *Ibam*	orthorhombic, *Ibam*	monoclinic, $P2_1/c$	monoclinic, $P2_1/c$
temperature (K)	293 K	293 K	293 K	293 K
a (Å)	11.6762(9)	11.6160(6)	5.1267(3)	4.8458(13)
b (Å)	9.9317(8)	9.8048(6)	9.7532(5)	9.045(2)
c (Å)	6.28060(19)	6.10915(14)	6.8070(2)	6.0624(8)
β (deg)	90	90	97.016(3)	92.279(10)
volume (Å^3)	728.33(8)	695.79(6)	337.82(3)	265.50(10)
D (g cm^{-1})	1.314	1.376	1.417	1.803
Z	8	8	4	4
R_{wp}	3.234	3.134	2.610	3.804

main $2\theta = 90°$ detector bank. The summed pattern was then normalized with respect to the incident beam monitor and the scattering from a spherical vanadium standard sample. Lastly, the diffraction pattern intensities were corrected for the wavelength and scattering-angle dependence of the neutron attenuation by the P-E cell anvil and gasket (Ti–Zr) materials. Sample pressures were calculated from the refined CaF_2 lattice parameters and the known room-temperature equation of state. Structures were refined in TopasAcademic using a Z-matrix model parametrized in terms of the intramolecular bond distances, angles, and torsions and the molecular position and orientation.[28] The starting models were derived from our previous X-ray diffraction study.[21] The DFT-optimized structures (see below) were used to formulate restraints which were then applied to the Rietveld refinements, as described in ref 29. Figure 1 shows two Rietveld fits of data at 0.32 GPa (phase I) and 0.87 GPa (phase II), and the corresponding crystallographic data for selected pressures is shown in Table 1. A plot of the diffraction at various pressures (Figure ES1) as well as the crystallographic information for all pressures (Table ES1) can be found in the Supporting Information. Figure 2 shows the changes in unit cell parameters and molecular volume with increasing pressure. The phase transition from phase I to phase II can clearly be observed at 0.8 GPa.

During the compression of acrylic acid, it was noted that the sample pressure continued to increase slowly after a finite change of pressure before eventually stabilizing after an interval of ~30 min. We have attributed this unusual behavior to the solubility of acrylic acid in the PTM and that during compression there is an initial solubilization of the acrylic acid before it recrystallizes back out of solution, causing the creep in pressure. This effect became less pronounced at higher pressures, which would be consistent with the expected decrease in solubility with pressure.

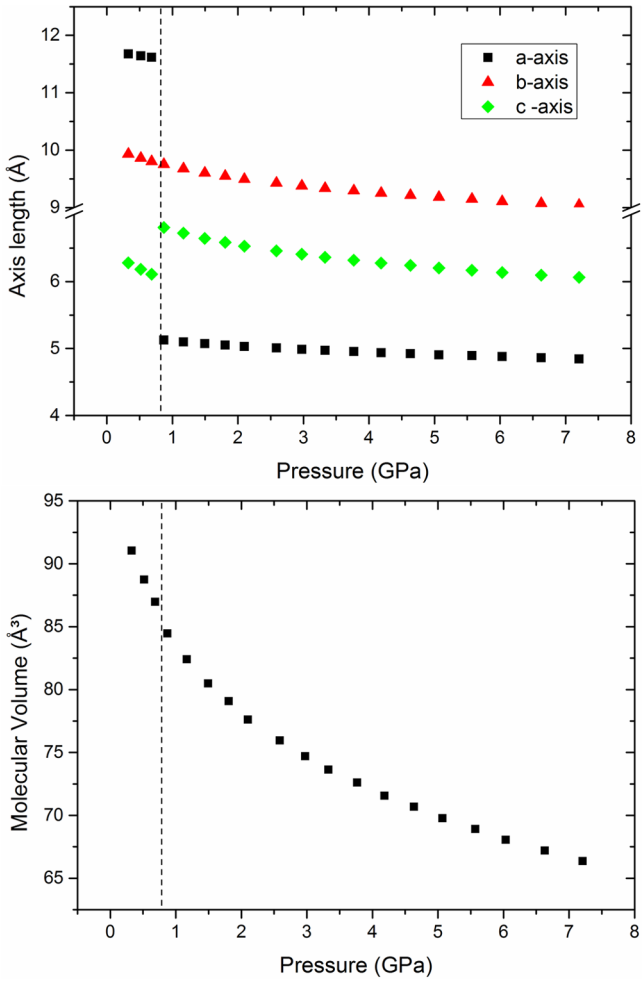

Figure 2. The unit cell parameters as a function of pressure (upper). The molecular volume of acrylic acid as a function of pressure (lower). The dotted line is representative of the phase boundary between the two phases.

Periodic DFT Calculations. Geometry optimizations were performed by periodic density functional theory (DFT) using the DMOL^3 code[30] as part of the Materials Studio modeling suite.[31] The DNP numerical basis set[30] was used in combination with the PBE functional[32] with the Tkatchenko–Scheffler correction for dispersion.[33] The unit cell dimensions were held fixed at the values obtained in Pawley refinements of the neutron powder diffraction data described above, and coordinates were allowed to optimize. Convergence was defined when the maximum changes in total energy, displacement, and gradient were 10^{-5} Ha, 5×10^{-3} Å, and 2×10^{-3} Ha Å^{-1}, respectively. Brillouin zone integrations were

dx.doi.org/10.1021/jp502095n | J. Phys. Chem. B 2014, 118, 4044–4051

performed by Monkhorst–Pack[34] k-point sampling at intervals of 0.07 Å^{-1}.

The Raman modes for acrylic acid-d_4 were calculated using the plane-wave-pseudopotential CASTEP v4.2 program[35] as implemented in Materials Studio,[31] employing the generalized gradient approximation (GGA) functional PW91[32] using the optimized phase I structure at 0.32 GPa. This cell was reduced to P1 before calculation. Norm-conserving pseudopotentials optimized for GGA DFT methods with a basis set cutoff energy of 830 eV were used. Brillouin zone integrations were performed with a 1,1,2 k-point set Monkhorst–Pack[34] grid. Lattice parameters remained fixed, but the atomic positions were optimized according to the following criteria: total energy convergence 5×10^{-6} eV/atom, maximum force on any atom 0.01 eV/Å, stress 0.02 GPa, and atomic displacements 5×10^{-4} Å.

Pixel Calculations. Using the optimized structures from the DFT calculations, the lattice energies and molecule–molecule interaction energies were calculated using the Pixelc module in the CLP package by Gavezotti.[36,37] Electron densities were calculated at the MP2/6-31G** level using Gaussian 09.[38] Calculation of the energies using the refined data showed a similar trend but not as smooth as those observed with the optimized structures highlighting the limitations of refining powder data even with the implementation of restraints; hence, the optimized structures were used. During the creation of the Z-matrix, bond lengths to deuterium atoms were normalized to neutron values and thus these values were retained for the energy calculations. Table ES2 (Supporting Information) provides the total lattice energy as well as the breakdown of intermolecular interactions into Coulombic, electrostatic, dispersion, and repulsion terms.

RESULTS AND DISCUSSION

The Effect of Pressure on Acrylic Acid-d_4. Acrylic acid phase I crystallizes in a layered structure, with the layers perpendicular to the c-axis (space group $Ibam$), where the acid groups hydrogen bond via a dimer motif (Figure 3); this is the same phase that is observed in the $-h_4$ system. The dimers are arranged in the layer so that the CD groups of C2 and C3 are in close contact with the oxygen atoms of a neighboring dimer. Pixel calculations of phase I show that by far the most favorable molecule–molecule interaction is, unsurprisingly, between the hydrogen bonded molecules (interaction 1) with the dispersive and Coulombic terms showing the greatest stabilizing contribution (Figure 4a; Table ES2, Supporting Information).

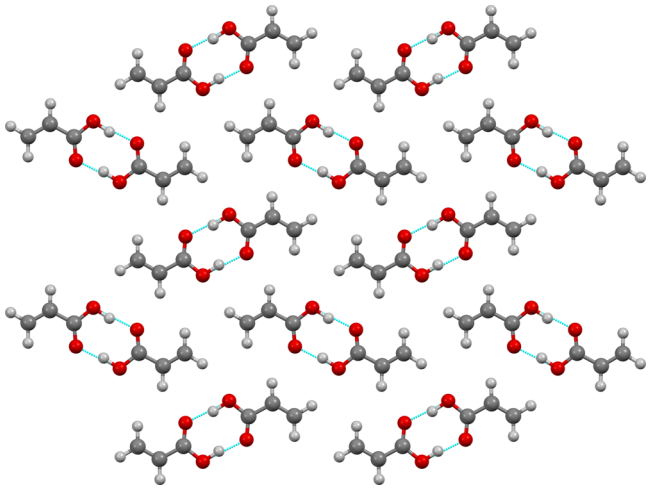

Figure 3. A layer of molecules lying perpendicular to the c-axis as observed in phase I and phase II of acrylic acid with the molecules hydrogen bonding through a typical carboxylic acid dimer. Atom colors are assigned as follows: gray, carbon; red, oxygen; white, hydrogen.

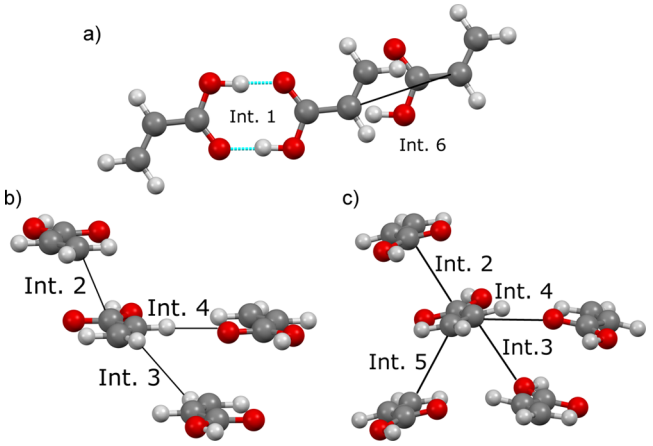

Figure 4. Six most imporatant interactions for the acrylic acid polymorphs: (a) Int. 1 is the carboxylic dimer that is observed in both phases. Int. 6 is observed only in phase II. (b) The interlayer interactions observed in phase I. (c) The interlayer interactions observed in phase II. Similar interactions have been identified between polymorphs and their descriptor kept constant despite the structural changes between phases, e.g., Int. 3. Atom colors are assigned as follows: gray, carbon; red, oxygen; white, hydrogen.

Interaction 2 represents the interaction between the central molecule and molecules directly above and below (in different layers) where the carbonyl groups of the acid are arranged in an antiparallel arrangement (Figure 4b). This type of interaction has been investigated for its potential stabilizing contribution to the crystalline state by Allen et al.[39] They showed through the use of the Cambridge Structural Database (CSD) and *ab initio* molecular-orbital calculations that carbonyl–carbonyl interactions can be comparable to medium-strength hydrogen bonds albeit that they are a little weaker in this case. While the energies calculated from Pixel cannot be broken down into individual interactions, there is a significant contribution from the dispersive component in interaction 2 which is known to contribute to carbonyl–carbonyl interactions. Interaction 4 is the second most attractive interaction displayed in phase I, where neighboring dimers in the layer interact through close contacts between the CD2 and CD4 with O1 and O2. Due to the layered nature of the structure, this interaction will be important as the acrylic acid is subjected to an applied pressure.

On compression to 0.69 GPa, the unit cell parameters of phase I compress by 0.5, 0.27, and 2.73% for the a-, b-, and c-axis, respectively, with the molecular volume reducing by 4.47% (Figure 2). Increasing the pressure to 0.86 GPa initiates a sluggish transition to a new phase (phase II, $P2_1/c$), similar to that of acrylic acid-h_4, which is complete after ~30 min. This pressure is slightly higher than was originally quoted in our previous paper of acrylic acid-h_4 (0.6 GPa,) but this may be due to either the different ratios of acrylic acid to PTM that was used in this study compared with our original study (20% v/v PTM this study; 50% v/v previous work), a deuteration effect, or the sample environment that has been used in this study.

dx.doi.org/10.1021/jp502095n | J. Phys. Chem. B 2014, 118, 4044–4051

The phase transition was also monitored in a diamond anvil cell (DAC) where the reconstructive nature can clearly be observed (Figure 5). The longer time for full conversion in the DAC (60 min) was probably due to the larger crystallites involved compared with the deliberately fine powder that is observed in the P-E cell during the neutron experiment; the quality of the powder was monitored indirectly through the analysis of the patterns from different detector banks.

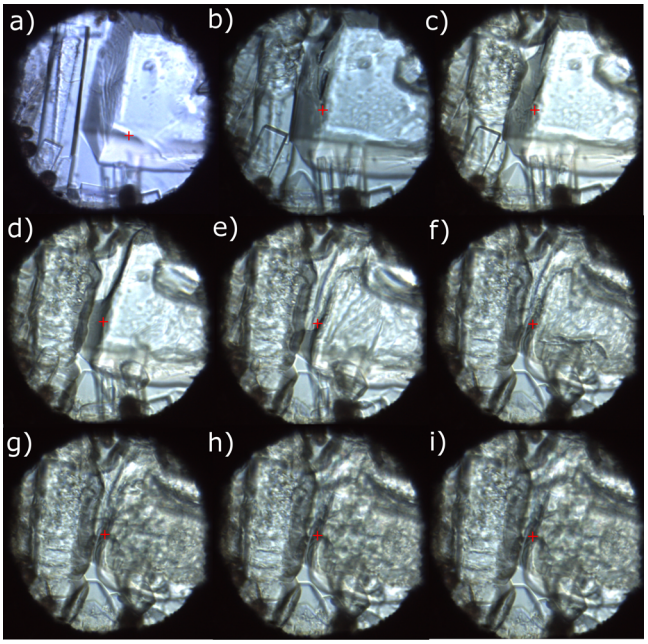

Figure 5. Images of the I−II transition in acrylic acid-d_4 observed in a diamond anvil cell taken at various times after a pressure increase to 0.8 GPa. The ruby spheres can be observed at the bottom of the gasket hole. (a) 0 min, (b) 12 min, (c) 18 min, (d) 26 min, (e) 30 min, (f) 40 min, (g) 48 min, (h) 56 min, and (i) 60 min.

Over the phase transition, the *a*-axis approximately halves, the *b*-axis maintains its compression rate, i.e. relatively unchanged, and the *c*-axis elongates. These changes to the unit cell result in a small change in the molecular volume (2.9% reduction; cf. 2.0% from 0.52 to 0.68 GPa in phase I), but it does lead to a significant reduction in the void volume from ∼30 to ∼4 Å^3 (as calculated by Materials Mercury).[40] This is an 87% reduction in void volume compared with a 47% reduction that is observed from 0.31 to 0.68 GPa in phase I.

The packing of molecules within the layers is similar in both phases, but in phase II, the layers are puckered and their relative positions with respect to neighboring layers also change. There is a 5.52, 7.26, and 10.94% compression of the *a*-, *b*-, and *c*-axes, respectively, that culminates in a 21.41% compression of the unit cell volume from 0.86 to 7.2 GPa. The bulk modulus for phase II was determined to be 6.6(7) GPa with a V_0 value of 371(3) Å^3 using a Murnaghan equation of state (EOS) in EoSFIT5.2.[41] The data were difficult to fit due to the compressibility of the material and the lack of low pressure data or reliable ambient pressure volume (acrylic acid is liquid under ambient pressure and temperature). These were the best values calculated from a number of different EOS (Birch−Murnaghan, Vinet and Murnaghan). The V_0 value seems reasonable given the molecular volumes of the two phases are very close to one another; hence, using the value at 0.33 GPa, one obtains a V_0 value of 364 Å^3. Up to this pressure, acrylic acid remains molecular and no polymerization occurs, consistent with the previously observed onset of polymerization at 8 GPa with loss of Raman modes.[20] We have also carried out Raman studies on the $-h_4$ form to 8.2 GPa, and we see little change in the spectrum except around the C—C torsion (∼350 cm^{-1}) and C═C—C bend (∼380 cm^{-1}) which may be signifying that the polymerization process is imminent.[21] Due to the experimental setup (ZTA anvils for a better signal-to-noise) and peculiar behavior of the sample, we were unable to compress the sample beyond 7.21 GPa.

The six most important molecular interactions (>4 kJ mol^{-1}) in phase II are shown in Figure 4, in which analogous interactions in phases I and II are illustrated. The interactions within the layers remain the same (interactions 1 and 4) even though neighboring dimers are now observed at a slight angle to each other due to the puckering of the layer. After the change of ∼10 kJ mol^{-1} over the phase transition, interaction 1 does not vary significantly until 4.1 GPa, where the total energy for the interaction starts to become more negative overall. At this point, there is an increase in the rate of change of the Coulombic term versus centroid distance, which may account for the effect on the overall energy of interaction. Toward 7.2 GPa, the energy of the interaction reaches a plateau, signifying that if the pressure were increased any further then either the repulsion between the molecules would overcome any attractive forces or the compression would be taken up elsewhere in the structure. A search of the CSD shows that the C1···C1′ (carbonyl carbon) distance observed at 7.2 GPa is at the minimum of those represented in the database, reflecting, perhaps, the lower limit that the hydrogen bonded dimer can be sustained before another molecular arrangement is required (Figure ES2, Supporting Information).

Interaction 2 still possesses an antiparallel interaction in phase II despite being in a slightly different orientation, which emphasizes the importance of this interaction in stabilizing the structure. As further pressure is applied to the structure, the total energy remains fairly constant before becoming less favorable at a value of ∼3.2 Å between the centroids of the molecules. In terms of the specific interaction between the carbonyl groups, the distance between the carbon and oxygen at this pressure is 3.15(5) Å, which is close to the energy minimum observed by Allen et al.[39] for this type of interaction (3.04 Å). Thus, while the Pixel calculations calculate molecule−molecule interactions, the trends in the energy associated with interaction 2 are consistent with previous literature detailing the interaction between carbonyl groups. Interaction 4 shows little change over the compression range. The total energy only starts to become more repulsive at ∼4.9 Å between the centroids, which equates to a contact distance of ∼2.16 Å between D2 and O2 which is somewhat surprising given that this interaction is within the layer and therefore should have less room for compression in comparison to interactions between the layers. Interaction 5, between molecules in different layers, shows the greatest change during the compression, with the overall energy changing by ∼13 kJ mol^{-1}. The molecules are aligned so that the alkene moieties are in close proximity to one another and thus will be associated with the polymerization reaction. The distance between the alkene groups compresses to 3.519 Å which is close to the optimal distance that is observed for polymerization reactions using diynes[16] and therefore is close enough to initiate the reaction.

dx.doi.org/10.1021/jp502095n | J. Phys. Chem. B 2014, 118, 4044−4051

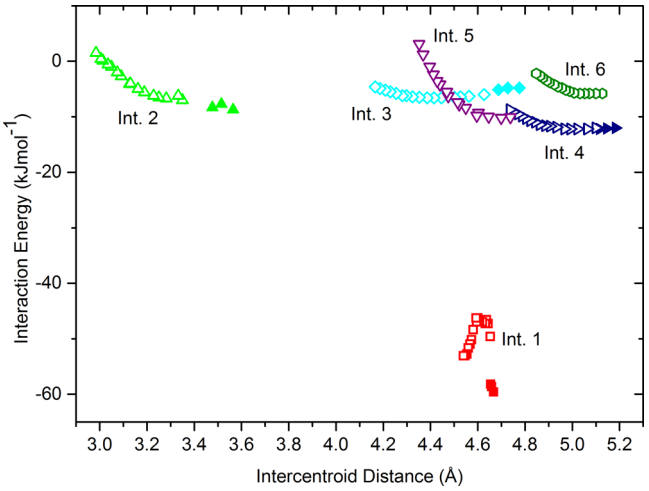

Figure 6. Plot of intercentroid distance and energy for each of the six highlighted interactions in phases I (filled symbols) and II (open symbols) of acrylic acid.

Raman Measurements of Acrylic Acid-d_4. The behavior of acrylic acid on decompression was not investigated using neutron diffraction; however, the experiment was repeated using Raman spectroscopy and a diamond anvil cell as the pressure vessel. Experimental details can be found in the Supporting Information. A few drops of the exact same solution of acrylic acid-d_4 in perdeuterated methanol:ethanol PTM were loaded into the DAC and compressed to 6.3 GPa (a similar pressure to the neutron experiment) (Figure 7, upper). The pressure was then held at this value overnight before decompression. This is significantly shorter than the neutron experiment; however, previous research by Murli and Song suggested that the high pressure phase was stable for over one month at 4.5 GPa.[20] The presence of the C═C stretch (1571 cm^{-1}) throughout the compression series shows that the molecular nature is retained to 6.3 GPa, which is consistent with the neutron data. This result also confirms that the energy of the laser used (532 nm) for pressure determination and Raman spectroscopy was not high enough to induce polymerization, as has been observed in other molecular systems at high pressure. Raman modes of the perdeuterated sample were calculated using CASTEP (Figure 7, upper) and show that deuteration has had a significant effect on the frequencies of specific stretches; e.g., the C═C bond, identified by Murli and Song, is at 1644 cm^{-1} for the hydrogenated sample, whereas we observe this frequency at 1571 cm^{-1} for the $-d_4$ sample.

On decompression, the sample remains in the molecular phase to 2.2 GPa; however, further decompression to 0.2 GPa shows a significant relative increase in the vibrations at 1635 and 1685 cm^{-1} when compared with the C═C stretch, indicating that polymerization has occurred. This delay in polymerization on decompression has been observed in other systems, such as benzene, where the reaction may be initiated at high pressure, but it is only on the release of pressure that sufficient volume is available for the reaction to reach completion.[5] The drop from 2.0 to 0.2 GPa straddles the I–II phase transition, which would also allow freedom for the molecules to move, thereby permitting polymerization to occur. We have conducted subsequent experiments where we have loaded the exact same sample from the neutron experiment into a diamond anvil cell, compressed it to 1 GPa, and left it at this pressure for a week. Even at this low pressure, the material had

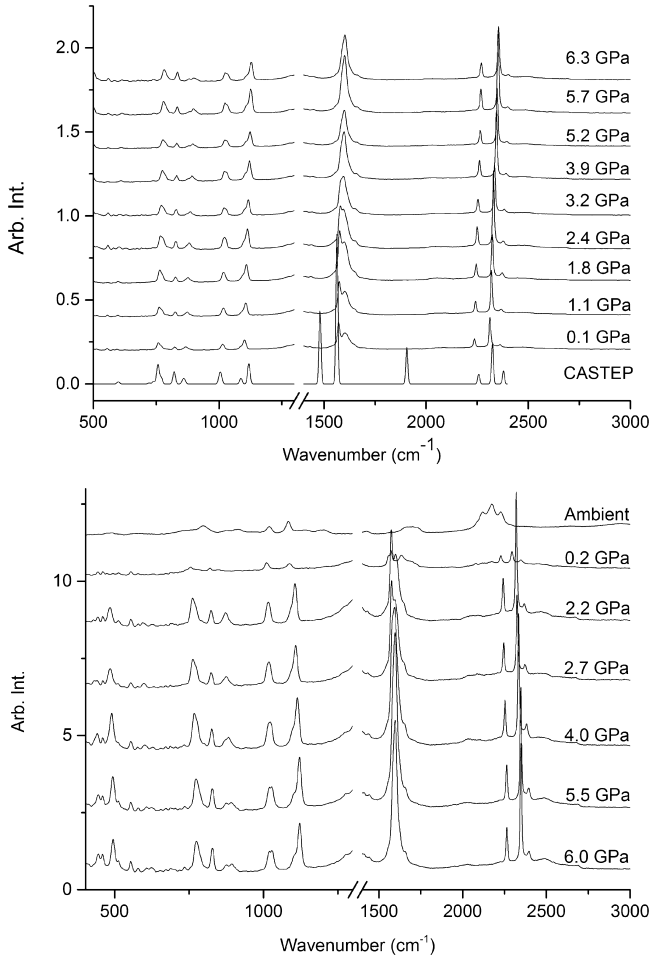

Figure 7. Raman spectra of acrylic acid-d_4 at various pressures on compression. The CASTEP spectrum was calculated using the 0.33 GPa data after geometry optimization (upper); Raman spectra on decompression (lower). Note the changes to the Raman peak at ~1635 and 1685 cm^{-1} between 2.2 and 0.2 GPa.

started to polymerize which would help to support our theory with respect to the polymerization mechanism.

FT-IR Measurements of Neutron Diffraction Product. Experimental details for the FT-IR measurements can be found in the Supporting Information. Upon opening the Ti–Zr gasket from the P-E cell neutron diffraction experiment, there was an odor of residual unreacted acrylic acid, but the vast majority was polymerized which bound together the other content of the capsule (CaF_2 and glass wool). Figure ES3 (Supporting Information) shows the IR spectrum of the product. The first observation is that there are stretches in both the C—D/O—D region (2250–2750 cm^{-1}) and the O—H region (3250–3750 cm^{-1}). The O—H stretch will be due to water present in the sample adsorbed after opening the gasket to the atmosphere due to the hygroscopic nature of poly(acrylic acid); PAA has been used as a hydrogel in the past.[42] The C═O stretch remains in a similar position to other PAA samples of different molecular weights (purchased from Sigma-Aldrich, Figure ES3, Supporting Information) (~1700 cm^{-1}); however, the stretch does not possess a shoulder toward higher wavenumbers that appears in the other higher molecular weight polymers. This may be due to a greater proportion of the acid moieties being engaged in hydrogen bonding; therefore, the environments around the carbonyl groups are less varied than in a polymer

dx.doi.org/10.1021/jp502095n | J. Phys. Chem. B 2014, 118, 4044–4051

produced through more conventional routes; i.e., the molecules are fully hydrogen bonded in the solid state, and this is translated into the polymer product. This would also affect the bands around 1178 and 1248 cm^{-1} which have been characterized as C—O stretching coupled with OH bending.[43] The polymer produced during the neutron experiment shows very small absorbances in this region compared with the high molecular weight polymers, but there is a more substantial absorbance between 800 and 1100 cm^{-1} that could be partially due to the C—O stretch in a highly hydrogen-bonded system but this assignment is cautious as the Si—O stretch from the glass wool also appears at ∼891 cm^{-1}.

Differential Scanning Calorimetry (DSC). Experimental details for the DSC measurements can be found in the Supporting Information. The sample from the neutron diffraction experiment was also analyzed via DSC. The sample was heated at a rate of 10 K min^{-1} from 300 to 650 K (Figure ES4, Supporting Information). The trace shows two main endothermic events at 330 and 503 K which represent dehydration and the formation of poly(acrylic acid) anhydride. These temperatures are in agreement with the study by Moharram and Allam,[44] indicating that, despite the observed changes in the Raman and IR, the thermal properties remain consistent with polymers synthesized by standard procedures.

CONCLUSIONS

We have confirmed that the acrylic acid-d_4 undergoes a polymorphic transition at ∼0.87 GPa using neutron diffraction. We have identified that acrylic acid retains its molecular nature up to a static pressure of 7.21 GPa but then undergoes polymerization between 0.2 and 2.2 GPa on decompression, which can be attributed to the increase in molecular volume that allows the polymerization reaction to proceed unhindered. We have also shown that one can also initiate polymerization by applying pressures of ∼1 GPa for a period of a week. The resulting products have been analyzed using IR, Raman, and DSC. While the DSC trace shows previously identified thermal events, the Raman and IR present peaks are different from those observed for polymers synthesized under conventional polymerization conditions, thereby indicating the novel polymeric structure obtained via high pressure techniques.

ASSOCIATED CONTENT

Supporting Information

Information relating to the experimental methods of Raman, IR, DSC, and Cambridge Structural Database searches. Figures of the powder neutron diffraction, IR, and DSC are shown. Tabulated information of the full crystallographic information and Pixel energies is also presented. This material is available free of charge via the Internet at http://pubs.acs.org.

AUTHOR INFORMATION

Corresponding Author

*E-mail: iain.oswald@strath.ac.uk. Phone: +441415482157.

Notes

The authors declare no competing financial interest.

ACKNOWLEDGMENTS

The authors would like to thank Andy Chamberlain for technical assistance during the PEARL experiment (RB1110228) and STFC for funding beamtime at ISIS Neutron Facility. The authors would also like to thank Dr Amit Delori for his help in producing the video and The Leverhulme Trust for funding RPG-2012-598.

REFERENCES

(1) Fabbiani, F. P. A.; Buth, G.; Dittrich, B.; Sowa, H. Pressure-Induced Structural Changes in Wet Vitamin B12. *CrystEngComm* **2010**, *12* (9), 2541−2550.

(2) Granero-Garcia, R.; Lahoz, F. J.; Paulmann, C.; Saouane, S.; Fabbiani, F. P. A. A Novel Hydrate of Alpha-Cyclodextrin Crystallised under High-Pressure Conditions. *CrystEngComm* **2012**, *14* (24), 8664−8670.

(3) Oswald, I. D. H.; Lennie, A. R.; Pulham, C. R.; Shankland, K. High-Pressure Structural Studies of the Pharmaceutical, Chlorothiazide. *CrystEngComm* **2010**, *12* (9), 2533−2540.

(4) Oswald, I. D. H.; Pulham, C. R. Co-Crystallisation at High Pressure - an Additional Tool for the Preparation and Study of Co-Crystals. *CrystEngComm* **2008**, *10* (9), 1114−1116.

(5) Bini, R.; Ceppatelli, M.; Citroni, M.; Schettino, V. From Simple to Complex and Backwards. Chemical Reactions under Very High Pressure. *Chem. Phys.* **2012**, *398*, 262−268.

(6) Chelazzi, D.; Ceppatelli, M.; Santoro, M.; Bini, R.; Schettino, V. Pressure-Induced Polymerization in Solid Ethylene. *J. Phys. Chem. B* **2005**, *109* (46), 21658−21663.

(7) Ciabini, L.; Santoro, M.; Bini, R.; Schettino, V. High Pressure Reactivity of Solid Benzene Probed by Infrared Spectroscopy. *J. Chem. Phys.* **2002**, *116* (7), 2928−2935.

(8) Santoro, M.; Gorelli, F. A.; Bini, R.; Ruocco, G.; Scandolo, S.; Crichton, W. A. Amorphous Silica-Like Carbon Dioxide. *Nature* **2006**, *441* (7095), 857−860.

(9) Aoki, K.; Kakudate, Y.; Yoshida, M.; Usuba, S.; Fujiwara, S. High-Pressure Raman-Study of a One-Dimensional Hydrogen-Bonded Crystal of Cyanoacetylene. *J. Chem. Phys.* **1989**, *91* (5), 2814−2817.

(10) Aoki, K.; Kakudate, Y.; Yoshida, M.; Usuba, S.; Fujiwara, S. Solid-State Polymerization of Cyanoacetylene into Conjugated Linear-Chains under Pressure. *J. Chem. Phys.* **1989**, *91* (2), 778−782.

(11) Ceppatelli, M.; Fontana, L. The High Pressure Reactivity of Substituted Acetylenes: a Vibrational Study on Diphenylacetylene. *Phase Transitions* **2007**, *80* (10−12), 1085−1101.

(12) Ceppatelli, M.; Santoro, M.; Bini, R.; Schettino, V. Fourier Transform Infrared Study of the Pressure and Laser Induced Polymerization of Solid Acetylene. *J. Chem. Phys.* **2000**, *113* (14), 5991−6000.

(13) Kojima, Y.; Matsuoka, T.; Sato, N.; Takahashi, H. High-Pressure Synthesis of Cyclic Phenylacetylene Oligomer. *J. Polym. Sci., Part A: Polym. Chem.* **1995**, *33* (17), 2935−2940.

(14) Santoro, M.; Ciabini, L.; Bini, R.; Schettino, V. High-Pressure Polymerization of Phenylacetylene and of the Benzene and Acetylene Moieties. *J. Raman Spectrosc.* **2003**, *34* (7−8), 557−566.

(15) Jin, H. J.; Plonka, A. M.; Parise, J. B.; Goroff, N. S. Pressure Induced Topochemical Polymerization of Diiodobutadiyne: a Single-Crystal-to-Single-Crystal Transformation. *CrystEngComm* **2013**, *15* (16), 3106−3110.

(16) Wilhelm, C.; Boyd, S. A.; Chawda, S.; Fowler, F. W.; Goroff, N. S.; Halada, G. P.; Grey, C. P.; Lauher, J. W.; Luo, L.; Martin, C. D.; et al. Pressure-Induced Polymerization of Diiodobutadiyne in Assembled Cocrystals. *J. Am. Chem. Soc.* **2008**, *130* (13), 4415−4420.

(17) Ceppatelli, M.; Frediani, M.; Bini, R. High-Pressure Reactivity of L,L-Lactide. *J. Phys. Chem. B* **2011**, *115* (10), 2173−2184.

(18) Murli, C.; Mishra, A. K.; Thomas, S.; Sharma, S. M. Ring-Opening Polymerization in Carnosine under Pressure. *J. Phys. Chem. B* **2012**, *116* (15), 4671−4676.

(19) Argade, A. B.; Peppas, N. A. Poly(acrylic acid) Poly(vinyl alcohol) Copolymers with Superabsorbent Properties. *J. Appl. Polym. Sci.* **1998**, *70* (4), 817−829.

(20) Murli, C.; Song, Y. Pressure-Induced Polymerization of Acrylic Acid: A Raman Spectroscopic Study. *J. Phys. Chem. B* **2010**, *114* (30), 9744−9750.

(21) Oswald, I. D. H.; Urquhart, A. J. Polymorphism and Polymerisation of Acrylic and Methacrylic Acid at High Pressure. *CrystEngComm* **2011**, *13* (14), 4503−4507.
(22) ISIS_Dedicated_Facility_for_High_Pressure_Diffraction *ISIS 96-ISIS Facility Annual Report 1995−96*; Rutherford Appleton Laboratory: 1996; pp 61−62.
(23) ISIS_PEARL_Pressure_and_Engineering_Research_Line *ISIS 97-ISIS Facility Annual Report 1996−97*; Rutherford Appleton Laboratory: 1997; pp 28−29.
(24) Ting, V. P.; Henry, P. F.; Schmidtmann, M.; Wilson, C. C.; Weller, M. T. Probing Hydrogen Positions in Hydrous Compounds: Information from Parametric Neutron Powder Diffraction Studies. *Phys. Chem. Chem. Phys.* **2012**, *14* (19), 6914−6921.
(25) Ting, V. P.; Henry, P. F.; Schmidtmann, M.; Wilson, C. C.; Weller, M. T. In Situ Neutron Powder Diffraction and Structure Determination in Controlled Humidities. *Chem. Commun.* **2009**, *48*, 7527−7529.
(26) Marshall, W. G.; Francis, D. J. Attainment of Near-Hydrostatic Compression Conditions using the Paris-Edinburgh Cell. *J. Appl. Crystallogr.* **2002**, *35*, 122−125.
(27) Besson, J. M.; Nelmes, R. J.; Hamel, G.; Loveday, J. S.; Weill, G.; Hull, S. Neutron Powder Diffraction above 10-Gpa. *Physica B* **1992**, *180*, 907−910.
(28) Coelho, A. *TOPAS − Academic: General Profile and Structure Analysis Software for Powder Diffraction Data*, version 5; Coelho Software: Brisbane, Australia, 2012.
(29) Funnell, N. P.; Dawson, A.; Marshall, W. G.; Parsons, S. Destabilisation of Hydrogen Bonding and the Phase Stability of Aniline at High Pressure. *CrystEngComm* **2013**, *15* (6), 1047−1060.
(30) Delley, B. An All-Electron Numerical-Method for Solving the Local Density Functional for Polyatomic-Molecules. *J. Chem. Phys.* **1990**, *92* (1), 508−517.
(31) Accelrys_Software_Inc, In *Materials Studio Release Notes, Release 6*, San Diego, CA, 2011.
(32) Perdew, J. P.; Chevary, J. A.; Vosko, S. H.; Jackson, K. A.; Pederson, M. R.; Singh, D. J.; Fiolhais, C. Atoms, Molecules, Soilds, and Surfaces- Applications of the Generalized Gradient Approximation for Exchange and Correlation. *Phys. Rev. B: Condens. Matter Mater. Phys.* **1992**, *46* (11), 6671−6687.
(33) Tkatchenko, A.; Scheffler, M. Accurate Molecular Van Der Waals Interactions from Ground-State Electron Density and Free-Atom Reference Data. *Phys. Rev. Lett.* **2009**, *102* (7), 073005.
(34) Monkhorst, H. J.; Pack, J. D. Special Points for Brillouin-Zone Integrations. *Phys. Rev. B* **1976**, *13* (12), 5188−5192.
(35) Clark, S. J.; Segall, M. D.; Pickard, C. J.; Hasnip, P. J.; Probert, M. J.; Refson, K.; Payne, M. C. First Principles Methods using CASTEP. *Z. Kristallogr.* **2005**, *220* (5−6), 567−570.
(36) Gavezzotti, A. Non-Conventional Bonding between Organic Molecules. The 'Halogen Bond' in Crystalline Systems. *Mol. Phys.* **2008**, *106* (12−13), 1473−1485.
(37) Gavezzotti, A. Calculation of Intermolecular Interaction Energies by Direct Numerical Integration over Electron Densities. 2. An Improved Polarization Model and the Evaluation of Dispersion and Repulsion Energies. *J. Phys. Chem. B* **2003**, *107* (10), 2344−2353.
(38) Frisch, M. J.; Trucks, G. W.; Schlegel, H. B.; Scuseria, G. E.; Robb, M. A.; Cheeseman, J. R.; Scalmani, G.; Barone, V.; Mennucci, B.; Petersson, G. A.; et al. *Gaussian 09*, revision B.01; Gaussian, Inc.: Wallingford, CT, 2009.
(39) Allen, F. H.; Baalham, C. A.; Lommerse, J. P. M.; Raithby, P. R. Carbonyl-Carbonyl Interactions can be Competitive with Hydrogen Bonds. *Acta Crystallogr., Sect. B* **1998**, *54*, 320−329.
(40) Macrae, C. F.; Bruno, I. J.; Chisholm, J. A.; Edgington, P. R.; McCabe, P.; Pidcock, E.; Rodriguez-Monge, L.; Taylor, R.; van de Streek, J.; Wood, P. A. Mercury CSD 2.0 - New Features for the Visualization and Investigation of Crystal Structures. *J. Appl. Crystallogr.* **2008**, *41* (2), 466−470.
(41) Angel, R. Equations of state. In *High-Temperature and High-Pressure Crystal Chemistry*; Mineralogical Society of America, Washington, D.C.
(42) Inoue, T.; Chen, G. H.; Nakamae, K.; Hoffman, A. S. A Hydrophobically-Modified Bioadhesive Polyelectrolyte Hydrogel for Drug Delivery. *J. Controlled Release* **1997**, *49* (2−3), 167−176.
(43) Dong, J.; Ozaki, Y.; Nakashima, K. Infrared, Raman, and Near-Infrared Spectroscopic Evidence for the Coexistence of Various Hydrogen-Bond Forms in Poly(acrylic acid). *Macromolecules* **1997**, *30* (4), 1111−1117.
(44) Moharram, M. A.; Allam, M. A. Application of Fourier Transform Infrared Spectroscopy to Study the Interactions of Poly(acrylic acid) and Mixtures of Poly(acrylic acid) and Poly-acrylamide with Bone Powders and Hydroxyapatites. *J. Appl. Polym. Sci.* **2007**, *105* (6), 3228−3234.